ASSESSING THE APPLICABILITY OF L-SHAPE ARRAY FOR MICROTREMOR SURVEY

LI Jinggang* **Supervisor: Toshiaki YOKOI****
MEE08156

ABSTRACT

Site effects play a major role in destructive ground motion. The effects of local geology may modify ground motion significantly on soft soils.To evaluate the site response, Microtremors methods have advantages: low cost and environment friendly for urban area and effective for low or moderate seismicity area. But standard array shape is strict circular. In urbanized area, it is usually very difficult to find an area for circular array observation due to existing buildings and other facilities. Therefore, irregular array should be investigated and in the paper L-shape array was checked by comparing the performances of circular array and L-shape array (both even and uneven interval) in the same site. The SPAC coefficients fit well with theoretical Bessel function, so the results are reliable. The results show that L-shape can have good performance in microtremors surveying. A shear wave profile was obtained by L-shape array and had good agreement with existing borehole data. The theory of Shiraishi et al.(2006) was attested by the observation data. Moreover, an effective and efficient method for the key step of SPAC analysis, frequency range selecting, was proposed.

Keywords: SPAC, L-shape array, Vs structure, Microremors

1. INTRODUCTION

China is one of the most earthquake-prone countries. Long time historical documents record these destructive earthquakes and huge number casualties, for which site effects is one of most important factors. The effects of local geology may amplify in a very significant way ground motion on soft soils.Most of Chinese people live in plain area with threat of potential earthquakes, and more and more people live in urban area with the urbanization of the world. So it is very important to evaluate the risk of strong ground motion. Microtremors method is a useful tool, but circular array sometimes is a strict constraint especially in urbanized area, where only L-shape array can be found. Shiraishi et al. (2006) proposed a new formula to deal with irregular arrays. The purpose of this study is to understand the effectiveness, limitations and advantages of L-shape array for the SPAC method using microtremors array measurement as a tool for seismic microzonation and earthquake disaster mitigation by applying them to a known old filled lake in Tsukuba City, comparing the results of them and then accessing the applicability of L-shape array.

2. METHODOLOGY

2.1 SPAC method with triangular array

Aki (1957;1965) proposed spatial autocorrelation method (or SPAC method) which exploited ambient vibration measurements to determine the underground shear wave velocity structure. Microtremors

*Institute of Seismology, China Earthquake Administration, China.
**International Institute of Seismology and Earthquake Engineering, Building Research Institute, Tsukuba, Japan.

mainly are treated as stationary surface waves. Under this hypothesis, the azimuthal average of real part of complex coherence function(CCF) (called the SPAC coefficient $\rho(r,\omega)$) equates to certain zero-order, first-kind Bessel function (Eq. (1)).

$$\rho(r_{AB},\omega)=\frac{1}{2\pi}\int_0^{2\pi}\frac{\mathrm{Re}\left(E[C_{A,B}(\omega)]\right)}{\sqrt{E[C_{A,A}(\omega)\cdot C_{B,B}(\omega)]}}d\theta \quad = J_0\left(kr\right), \tag{1}$$

2.2 Formulation of Shiraishi et al. (2006) for arbitrary shape array

According to the theory of Shiraishi et al. (2006), the real part of CCF can be expressed by taking finite terms as Eq. (1) due to drastic attenuation of higher order within range of interest.

$$\begin{aligned}\mathrm{Re}\left\{\left(\gamma_z\right)_{ij}\right\} &= J_0\left(kr_{ij}\right)+2\sum_{n=1}^{\infty}\left[\left(-1\right)^n J_{2n}\left(kr_{i,j}\right)\cdot\sum_{l=1}^{L}\lambda_{ij,l}\cos 2n\left(\theta_l+\phi_{ij}\right)\right]\\ &= J_0\left(kr_{ij}\right)-2J_2\left(kr_{ij}\right)\left\{\cos 2\phi_{ij}\sum_{l=1}^{L}\lambda_l\cos 2\theta_l-\sin 2\phi_{ij}\sum_{l=1}^{L}\lambda_l\sin 2\theta_l\right\}\\ &\quad+2J_4\left(kr_{ij}\right)\left\{\cos 4\phi_{ij}\sum_{l=1}^{L}\lambda_l\cos 4\theta_l-\sin 4\phi_{ij}\sum_{l=1}^{L}\lambda_l\sin 4\theta_l\right\}\\ &\quad-2J_6\left(kr_{ij}\right)\left\{\cos 6\phi_{ij}\sum_{l=1}^{L}\lambda_l\cos 6\theta_l-\sin 6\phi_{ij}\sum_{l=1}^{L}\lambda_l\sin 6\theta_l\right\}+O\left(J_8\left(kr_{ij}\right)\right),\end{aligned} \tag{2}$$

For equi-lateral triangular array, the real part of CCF was obtained by substituting $\phi_{01}=0°$, $\phi_{02}=60°,\phi_{03}=120°;r_{01}=r_{02}=r_{03}$ into Eq. (2).

$$\begin{aligned}\rho_L\left(\omega,r_{01}\right)=\frac{\mathrm{Re}\left\{\left(\gamma_z\right)_{0,1}\right\}+\mathrm{Re}\left\{\left(\gamma_z\right)_{0,2}\right\}+\mathrm{Re}\left\{\left(\gamma_z\right)_{0,3}\right\}}{3} &= J_0\left(kr_{01}\right)-2J_6\left(kr_{01}\right)\left\{\sum_{l=1}^{L}\lambda_l\cos 6\theta_l\right\}+O\left(J_8\left(kr_{01}\right)\right)\\ &= J_0\left(kr_{01}\right)+O\left(J_6\left(kr_{01}\right)\right).\end{aligned} \tag{3}$$

For L-shape array , we get the real part of CCF by substituting $\phi_{01}=0°,\phi_{02}=90°,$ $r_{01}=r_{02}$ into Eq. (2) respectively and obtain Eq. (4).

$$\rho_L\left(\omega,r_{01}\right)=\frac{\mathrm{Re}\left\{\left(\gamma_z\right)_{0,1}\right\}+\mathrm{Re}\left\{\left(\gamma_z\right)_{0,2}\right\}}{2}=J_0\left(kr_{01}\right)+J_4\left(kr_{01}\right)\left\{2\sum_{l=1}^{L}\lambda_l\cos 4\theta_l\right\}+O\left(J_8\left(kr_{01}\right)\right). \tag{4}$$

Naturally, the average of two pairs that form the short sides can reduce the influence of J_2(kr) term drastically, where as the oblique side follow Eq.(2) and suffers this influence.

In this paper, we use Common Middle Point Cross-correlation (CMPCC) method (Hayashi and Suzuki, 2004) to analyze MASW8 and MASW9. Combination of the Down Hill Simplex Method and the Very Fast Simulated Annealing (VFSA) method is used to find optimal values of Vs structure and layer depths, based on least misfit values between the observed and computed dispersion curves. The combination of these two methods drastically shortens the time consumption in comparison with the conventional VFSA(Yokoi,2005).

3. **DATA**

3.1 Observation site

We conducted a field observation of microtremors in Tsukuba city, Ibaraki Prefecture, located on the northern outskirts of Tokyo. The subsurface soil profile is well documented using PS logging records (geological columns and SPT data) and geological documents (Unozawa et al., 1988).

3.2 Array deployment and data acquisition

Totally 21 seismic sensors(natural frequency 2Hz), portable recording systems "GEODE" manufactured by Geometrics Corporation with the available frequency range from 1.75Hz to 20KHz, are used for microtremors observation. 24 geophones (natural frequency 4.5Hz) are deployed for multichannel analysis of surface waves (MASW).The map view of observation site is shown (Fig. 1).

Table 1. Array information

Array symbol	**Array type**	**Duration**	**remarks**
MAM1	Put together on the horizontal ground	65 seconds each time, 5 times	Huddle test(21 vertical component sensors)
MAM2	Triangular array	65 seconds each time, 30 times	19 vertical component sensors
MAM3	Even interval L-shape		11 vertical component sensors
MAM4	Uneven interval L-shape		
MAM5			
MAM6			
MAM7			
MASW8	MASW Linear array	2 shots	24 geophones
MASW9			

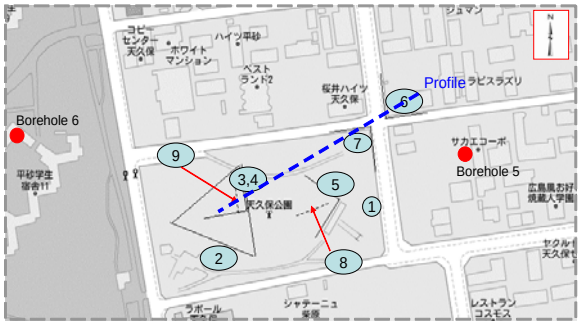

Figure 1. Observation site map view. Numbers with ellipse indicate different arrays and hereafter in the report and analysis these numbers with prefix "MAM" for microtremors method and "MASW" for MASW method are used to represent these arrays and their results. We put arrays with different methods (MAM2, MAM3, MAM4 and MASW9; MAM5 and MASW8) in the same site. The nearest borehole locations are also showed with red filled circles. Borehole data will be employed to check the results from profile crossing arrays MAM 6, MAM 7, MAM 5, and MAM 3 indicating by dashed line.

Table 2. Inter-station distance range for different arrays in experiment

	With/without oblique sides	Min. of inter-station distance(m)	Max. of inter-station distance(m)
Triangular array	\	2	60.6
Even interval L-shape array	with	6.0	42.4
	without	6.0	30.0
Uneven interval L-shape array	with	2.0	32.0
	without	2.0	45.3

Table 2 shows parameters of triangular array(MAM2) and L-shape array(even and uneven interval).Numbers of inter-station pairs of each inter-station distance of even and uneven interval arrays are 19 and 25 with oblique sides and 5 and 10 without oblique sides respectively. Although some of the inter-station distances have many inter-station pairs, azimuths of inter-station pairs are mainly within limited azimuth, which may import error of higher order Bessel function into SPAC

coefficients from theory of Shiraishi et al.(2006). Without oblique sides, there is obviously influence of 4-order Bessel function for both even and uneven L-shape arrays.

4. RESULTS AND DISCUSSION

We filtered the observation data with Chebyshev-I band-pass causal filter(parameters: FL=0.1Hz,FH=20.0Hz, FS=25.0Hz, AP=0.1,AS=10.0), and then new sampling interval is 0.02 second. Block size of analysis is 256, and the frequency range of analysis is [1.75-25Hz]. From the whole length, 65 seconds, of the array seismograms, we extracted data segments of duration 5.12 s with overlapping ratio 0.05. Then, for each of the blocks, the spectral densities were calculated by FFT. Those spectral densities were then each smoothed with a Parzen window of bandwidth 0.7 Hz, and were averaged over all data segments before they were used to estimate the inter-sensor correlations.

4.1 Determination of frequency range for analysis

It is very difficult to determine automatically and steadily by computer and time-consuming to determine frequency range by hand. The start and end points of the frequency range carefully picked by hand for each inter-station distance and then fitted with two exponential functions. The end points of frequency range fitted very well with root mean square (rms) error less than 0.5 and the start points of the range frequency range were less precise but still have a rms error less than 1.5 Hz ,

$$freq\_start = \frac{20}{dist^{0.5}}, \qquad freq\_end = \frac{35}{dist^{0.6}}, \tag{5}$$

where

$freq\_start$, $freq\_end$ — start point and end point of frequency range(unit: Hz),

$dist$ — inter-pair distance(unit: m).

4.2 Comparison of different methods at the same site

Equi-lateral triangular, even and uneven L-shape array for microtremors method and linear array for MASW method were conducted at the same site in the western part of Amakubo Park to check the validity of L-shape array. MASW is used to complement the performance of SPAC method. According to Shiraishi et al.'s theory, equi-lateral triangular has highest accuracy in these arrays with similar size array, which is viewed as a standard. From Figure 2, we can see:

(i) The triangular array(MAM2) combined with MASW9 is standard for comparison over broad frequency range [2-24Hz](written as MAM29)

(ii) Even interval L-shape array(MAM3) have frequency range [3.5-11Hz] both with and without oblique sides;

(iii) Uneven interval L-shape array MAM4 has frequency range [3.5-21Hz] and [3-21Hz] for with and without oblique sides. These frequency ranges are consistent with corresponding inter-station distance ranges.

(iv) Compared with MAM29, uneven interval array (MAM4) has higher accuracy then even one (MAM3) both with and without oblique sides. Moreover, dispersion curves of L-shape array without oblique side (MAM3ST and MAM4ST) are have less deviation from the standard one MAM29, which indicates that oblique sides import higher order Bessel function error into SPAC coefficients.

(v) Vs structures show similar results as dispersion curves, even interval array in the experiment is better than uneven one. Uneven interval array shows good agreement with MAM29, while even one has relatively large bias.

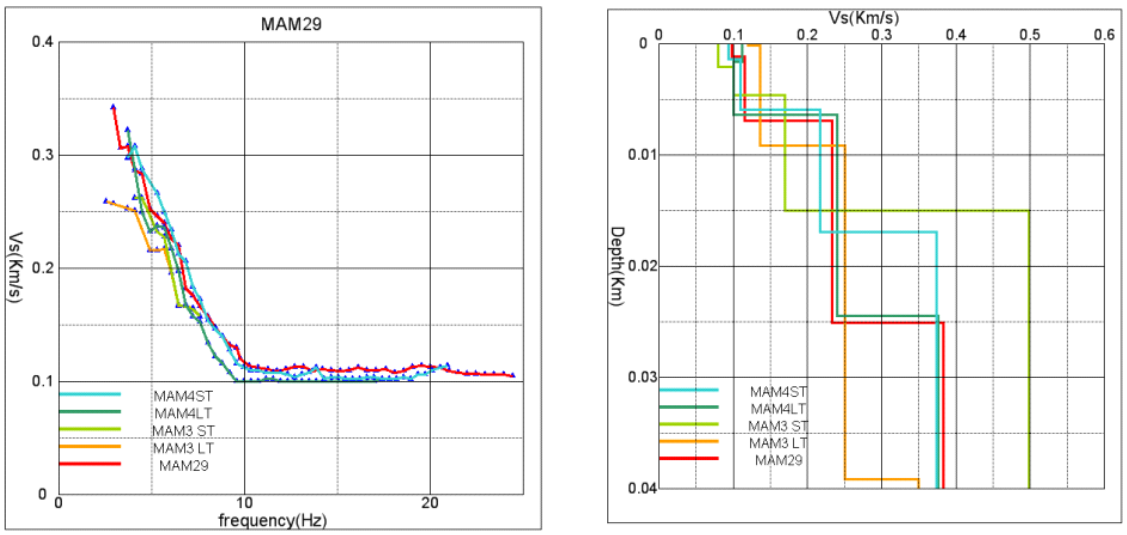

Figure 2. Dispersion curves(Left panel) and inverted Vs structures (Right panel)of MAM2, MAM3, MAM4 and MAM29 (combination of MAM2 and MASW9). Suffix "LT" and "ST" for MAM3 and MAM4 mean data of L-shape with and without oblique sides, respectively.

4.3 Results from even and uneven interval L-shape array

The frequency range of both with and without oblique sides of even L-shape array MAM3 is [2-12Hz] and that of uneven interval L-shape array MAM4 is [2-20Hz]. So with the same field effort, uneven array is advantageous over even one.

Usually we want to increase the number of observation to cancel out or minimize the random errors, so it is natural to use as many sensor pairs as possible to get the dispersion curves.

For L-shape, using sensor pairs of oblique sides may import influence of the 2nd order Bessel function because of giving too much weight to some directions, at the same time averaging of two short sides of L-shape array can remove the influence of 2nd order Bessel function. So it is necessary to check whether it is appropriate to include the oblique sides or not.

Both dispersion curves and Vs structures show that L-shape with and without oblique sides have similar performance. Furthermore, oblique sides have wider inter-distance range and hence wider frequency range.

4.4 Vs profile by Microtremors methods

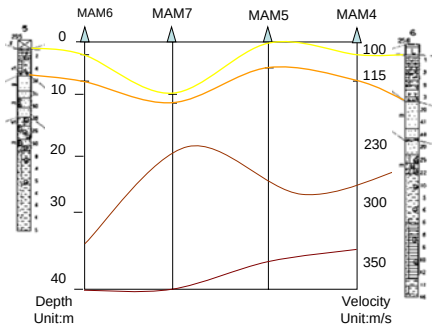

Figure 3. Vs profile through MAM6, MAM7, MAM5 and MAM4

Figure 3 shows the Vs profile determined by MAM6, MAM7, MAM5 and MAM4. This profile is in between Borehole 5 and Borehole 6. Left side numbers show the depth of each layer, and the right side ones indicate the shear wave velocity of each layer. Layers of the profile have good conformability with those of Borehole 5 and Borehole 6. The results show that microtremors method at frequency range [2-12Hz] can detect 20m with some accuracy.

5. CONCLUSIONS

1. Empirical formulas from fitting method can also provide reasonable frequency range.The formulas for the inter-station distance less than 60m are as follow respectively.

$$freq\_end = \frac{35}{dist^{0.6}} \quad and \quad freq\_start = \frac{20}{dist^{0.5}}$$

2. As far as analysis method of simple averaging of different azimuth, triangular array has higher accuracy than L-shape array, especially in the low frequency range.
3. Multichannel analysis of surface waves method has advantages in higher frequency, while triangular arrays have good performance in relatively low frequency range. Combination of these two can provide better constraint on Vs structure. Actual data of our experiment attest it.
4. For L-shape, uneven interval array has wider range of inter-station distance, then wide frequency range. Also, uneven interval array has more inter-station distance, which provides smoother dispersion curves.
5. Including oblique side sensor pairs in analysis can diminish stochastic error, but at the same time, it can import second order Bessel function $J_2(kr)$. Data of our experiments show that there seems to be no higher modes imported. Another advantage is that with oblique side we can get wider frequency range, because they have more and wider inter-station distances.
6. Microtremors method can provide shallow Vs profile for site effect evaluation up to about 20 m.
7. The theory of Shiraishi et al.(2006) is appropriate for identifying higher order Bessel function as a deviation to ideal circular array.

ACKNOWLEDGEMENT

I would like to express my sincere gratitude to Dr. Koichi Hayashi, OYO Corp. for his help during field work.

REFERENCES

Aki, K., 1957, Bulletin of the Earthquake Research Institute, 35, 415–456.
Aki, K., 1965, Geophysics, 30, 665–666.
Arai, H., and K. ,Tokimatsu, 2004, Bull. Seism. Soc. Am. 94, 53 –63.
Asten, M.W., and J.D., Henstridge, 1984, Geophysics, 49, 1828–1837.
Capon, J., 1969, Proceedings of the Institute of Electrical and Electronics Engineers, 57, 1408–1418.
Cho, I., T. Tada, and Y. Shinozaki, 2008, J. Geophys. Res., 113, B06307, doi: 10.1029/2007JB005245
Hayashi, K., H., Suzuki, 2004, Exploration Geophysics, 35, 7–13.
Ingber, L., 1989, Mathl. Comput. Modelling, 12, 967-973.
Miller, R.D., et al, 1999, The Leading Edge, 18, 1392-1396
Nelder, J. A., and R., Mead, 1965, Computer Journal, vol 7, pp 308-313.
Okada, H., 2003, Geophysical Monograph Series, No.12, Society of Exploration Geophysicists.
Shiraishi, H., et al, 2006, Geophys. Res. Lett. 33, L18307, doi: 10.1029/2006GL026723.
Unozawa, A., et al., 1988,Environmental Geologic Map of Tsukuba Science City and Its Surroundings Scale 1:25,000, Geological Survey of Japan.
Yokoi, T., 2005, Programme and abstracts, The Seismological Society of Japan, Fall meeting.
Yokoi. T. and S., Margaryan , 2008, Geophysical Prospecting, 56, 435-451.